A frequency-stabilized difference frequency generation laser spectrometer for precise line profile studies in the midinfrared

Wen-Ping Deng, Bo Gao, Cun-Feng Cheng, Guo-Sheng Cheng, Shui-Ming Hu,[a)] and Qing-Shi Zhu

Department of Chemical Physics, Hefei National Laboratory for Physical Sciences at the Microscale, University of Science and Technology of China, Hefei 230026, People's Republic of China

A midinfrared laser spectrometer is built up based on the difference frequency generation (DFG) of a Nd:YAG (yttrium aluminum garnet) laser and a tunable Ti:sapphire (Ti:Sa) laser. Tuning the Ti:Sa laser and operating properly with the periodically poled lithium niobate crystal, the DFG emission is tunable in the spectral range of $2.3-5.0$ μm. The 1064 nm Nd:YAG laser frequency is stabilized to the 10^{-6} cm^{-1} level on a Doppler-broadened I_2 absorption line at 532 nm. As a result, the DFG emission frequency is stabilized within 1×10^{-4} cm^{-1}. The measurement of an absorption line of CH$_4$ near 3 μm demonstrates that the DFG spectrometer is very suitable for the molecular absorption line profile studies in the midinfrared region. © *2008 American Institute of Physics.* [DOI: 10.1063/1.3033164]

I. INTRODUCTION

Many small molecules have strong fundamental absorption bands in the mid-infrared (mid-IR).[1] As a result, many applications are based on the molecular spectroscopic data in this region. The molecular spectral line profile data are essential in the studies of the atmospheric absorption modeling[2] and the investigations of the intermolecular interactions.[3,4] Recently Yamada *et al.*[5] reported the very precise molecular line profile measurement utilizing a frequency comb spectrometer operating in the near-infrared (near-IR) region. Daussy *et al.*[6] proposed to determine the Boltzmann constant from the precise measurement of the Doppler linewidth of a molecular line in the mid-IR region. For the purpose of line profile studies, a frequency precision at the level of 10^{-3} cm^{-1} or higher is necessary, which is beyond the possible spectral resolution of the available dispersion spectrometers or Fourier transform interferometers. In this case, spectroscopy based on tunable lasers will be the best choice. However, the commercially available mid-IR lasers are still quite limited if compared to those available in the near-IR and visible regions. Now the most commonly used mid-IR laser sources include CO/CO$_2$ gas lasers, lead-salt diode lasers, and quantum cascades.[7] However, most of them are very expensive and/or inconvenient compared with the widely used near-IR solid state lasers. The frequency-stabilized continuous wave (cw) mid-IR laser spectrometers for molecular line profile studies have been built in a few laboratories, for example, as in Refs. 8 and 9. They are both based on tunable diode laser working at liquid-nitrogen temperature, the tunable spectral ranges are also quite limited (tens of wavenumbers). The sideband emission as a background of the main lasering mode in such lasers is also a problem in the quantitative spectroscopy measurements.[3]

Another kind of choice to obtain the mid-IR laser emissions is the frequency conversion technique including difference frequency generation (DFG) and optical parametric oscillator (OPO).[7] They both utilize the nonlinear optical materials to get the mid-IR radiations from the well developed near-IR or visible laser sources. No need of cryogenic handling, large spectral coverage (typically $2-5$ μm) and relatively easy maintenance are the main advantages of the DFG and OPO methods. To date, the available cw-OPO system can produce up to 1 W IR emission while the emission power from a DFG system is less than 1 mW. However, the DFG configuration is simpler than the cw-OPO system, thus the operation and maintenance are easier. Meanwhile, mode-hop-free operation with good frequency stability is still a practical problem for the present cw-OPO system.[7] As will be presented in this work, a very important advantage over the cw-OPO system is that the DFG system can be operated with very high frequency stability by stabilizing the near-IR laser sources. In this way, the DFG system is attractive in the precision measurements in the mid-IR region. Vitcu *et al.*[10] reported line shape studies based on the DFG from two visible lasers (an argon ion laser and a dye laser).[4] Here we will present our mid-IR DFG laser spectrometer using a Ti:Sa laser and a Nd:YAG (yttrium aluminum garnet) laser. As will be discussed in Secs. II A–II D, the superior quality of the solid state near-IR lasers allows us to apply the DFG spectrometer for precise line profile measurement in a large mid-IR region.

II. EXPERIMENT

A. The difference frequency generation

The configuration of the DFG system is shown in Fig. 1. The cw mid-IR DFG radiation is obtained by mixing the near-IR beams from a tunable Ti:Sa laser and a single frequency Nd:YAG laser in a nonlinear periodically poled

---
a)Electronic mail: smhu@ustc.edu.cn.
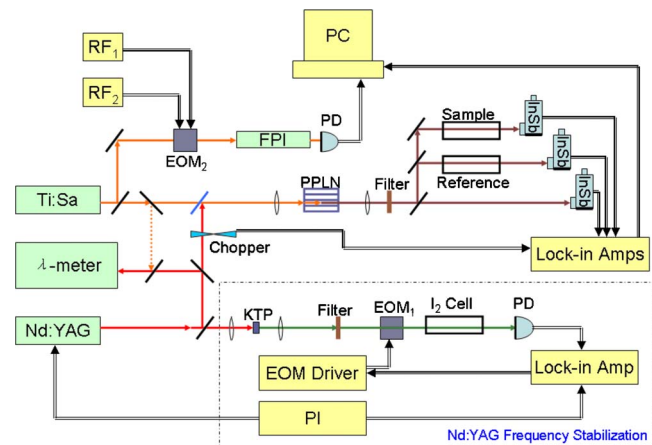
     79, 123101-1

FIG. 1. (Color online) The configuration of the mid-IR DFG spectrometer. Ti:Sa is Ti:sapphire laser; PPLN is periodically poled lithium niobate nonlinear crystal; FPI is Fabry–Pérot interferometer; EOM is electro-optic modulator; rf is radio frequency source; KTP is $KTiOPO_4$ crystal.

lithium niobate (PPLN) crystal. The Ti:Sa laser (Coherent 899-29) is pumped by a single mode 532 nm solid state laser (Coherent Verdi-10) and is tunable in the region 700–900 nm. The Nd:YAG laser (Innolight Mephisto 2000) can be tunable over several gigahertz around 1064 nm through the built-in piezoelectric transducer (PZT) and/or temperature controller of the laser.

The near-IR beams are cofocused and superimposed in the PPLN crystal (Crystal Technology Inc.). Each crystal is 20 mm long and has several channels with different poling periods. The crystal is mounted on a copper stage which is temperature stabilized by a feedback controller (± 0.1 K). When tuning the frequency, the PPLN crystal temperature is adjusted to fulfill the quasi-phase-matching conditions.[11,12] Comparing with the critical phase-matching birefringent crystals such as $AgGaS_2$ and $LiIO_3$, PPLN has higher conversion efficiency,[13] tilting the crystal and the "walk-off" effects can be also avoided in the tuning.[14] By tuning the Ti:Sa laser in the 700–900 nm region and selecting crystal channels with different poling periods varying from 18 to 23 μm, the frequency of the DFG emission can be tunable in the whole 2.3–5.0 μm region. With inputs of the Ti:Sa and Nd:YAG lasers of about 400 mW and 1.5 W, respectively, the output DFG emission power is around tens of microwatt. A bandpass filter is used to block the near-IR beams.

The frequency of the Ti:Sa laser is monitored with a λ-meter (Burleigh WA1500) and a Fabry–Pérot interferometer (FPI) (Thorlabs FPI100). The DFG emissions pass through the reference and sample cells, respectively, and then are detected by InSb detectors cooled with liquid nitrogen. The Nd:YAG laser is chopped with a mechanical chopper at about 2 kHz frequency and the DFG signals are demodulated with a lock-in amplifier (SRS SR830). The analog outputs from the lock-in amplifier and the FPI are digitized with an analog to digital converter card (NI PCI-6221) installed in a personal computer (PC).

B. Nd:YAG laser frequency stabilization

The linewidth of the Ti:Sa laser can be as narrow as 0.5 MHz, and the stated linewidth of the Nd:YAG laser is also below 1 MHz. However, the Nd:YAG laser has a stated long-term frequency drift of about 1 MHz/min and frequency jitters can be observed during the measurements. Such frequency drifts and jitters will transfer to the DFG emission and it prevents the precise line profile measurements. The frequency-stabilized 1064 nm Nd:YAG laser is often used for frequency standard purpose, where it is stabilized with the frequency modulation transfer technique[15] or the third-harmonic modulation technique[16] utilizing the strong iodine absorption lines near 532 nm. In those reports, the frequency of the Nd:YAG laser can be routinely locked to the subkilohertz level ($\delta \nu / \nu \sim 10^{-12}$). In our measurements, such an extremely high stability of the Nd:YAG laser is not essential, but the long-term drift must be avoided, so we use the Doppler-broadened absorption line to stabilize the Nd:YAG laser. Comparing with the stabilization method using the saturation spectroscopy, such method needs less input laser power, and provides wider dynamic range. Such advantages fit the needs in the present study.

The configuration of the Nd:YAG frequency stabilization is also presented in Fig. 1. Part of the Nd:YAG laser beam is used for frequency doubling using a $KTiOPO_4$ crystal. With about 100 mW 1064 nm laser beam input and a single pass in the crystal, about 5 μW of the 532 nm beam can be obtained. The 532 nm laser beam is modulated with a resonant electro-optic modulator (EOM) (EOM1, New Focus 4421) and then passes through the I_2 cell (Thorlabs CQ19100-I). The resonant radio frequency EOM driver (New Focus 3363) is amplitude modulated at 60 kHz, which is also used as the reference to demodulate the signal from the photodiode detector with a lock-in amplifier (EG&G 7260). By adjusting the temperature of the Nd:YAG laser, the frequency doubled laser beam is tuned at the iodine absorption line P(53)32–0 (18 788.424 cm^{-1}). The output of the lock-in amplifier is used as the error signal to the proportional-integral (PI) controller (SRS SIM960). The feedback signal from the PI is then amplified with a high-voltage amplifier (New Focus 3211) and finally used to drive the built-in PZT in the Nd:YAG laser to close the loop.

Figure 2(a) presents the frequency drifts when the stabilization loop is turned off and on, respectively. It can be seen from that figure, within 600 s measuring time that the error signal amplitude (corresponding to the frequency drift) drops dramatically when the feedback loop is closed. The actual frequency drift can be estimated from the slope of the spectrum at the locking point and the amplitude of the error signal. In this way, the Allan variances $\sigma^2(\tau)$ (Ref. 17) of the laser frequency drift can be obtained. Figure 2(b) shows the frequency stability described by the square root of Allan variance $\sigma(\tau)$. It can be seen from Fig. 2(b) that the frequency drift of the free-run 1064 nm Nd:YAG laser reaches over 10 MHz and the value decreases to the 0.01 MHz level when the stabilization loop is turned on.

We also tried to lock the Nd:YAG laser by adding a kHz modulation on the built-in PZT in the laser. Almost the same frequency stability has been achieved. This method is easier and does not need the expensive EOM, but it superimposes a small modulation on the DFG emission. In turn, the present method using EOM is modulation-free to the DFG output.
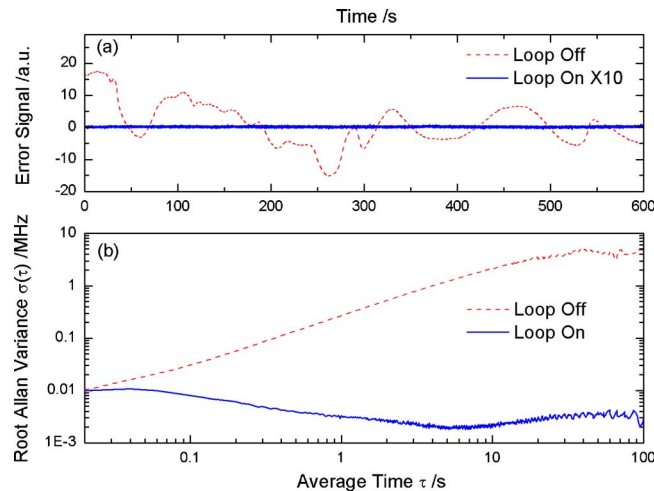
FIG. 2. (Color online) Frequency stability of the 1064 nm Nd:YAG laser. (a) Frequency drifts when the stabilization loop is off (free run, dash line) and on (solid line). (b) Frequency stability described with the root Allan variance $\sigma(\tau)$.

We have tested that the stabilization of the Nd:YAG laser can easily be maintained for all day, which is favorable for the long time measurements.

In this way, the Nd:YAG laser is stabilized at about 9394.21 cm^{-1}. To test the frequency stability of the DFG emission, the Ti:Sa laser is tuned at around 12 321.28 cm^{-1} to measure the CH$_4$ line at 2927.0762 cm^{-1} [the $P(9)$ line of the ν_3 band[18]]. The Ti:Sa laser frequency is locked by the factory provided internal stabilizing loop. The Ti:Sa laser frequency is manually placed at the right position so that the frequency of DFG emission is just at the waist of the CH$_4$ line. Then the fluctuations of the absorption signal will provide a measure of the frequency drift of the DFG emission. The observed frequency drift is shown in Fig. 3. When the Nd:YAG stabilization loop is turned off, in a 600 s long measurement, the DFG frequency drift is larger than 50 MHz (dash line, peak to peak), and it drops to about 4 MHz (1.3×10^{-4} cm^{-1}) when the loop is turned on (solid line). Such residual drift should mainly come from the Ti:Sa laser. Averaging the data in a proper time interval will further increase
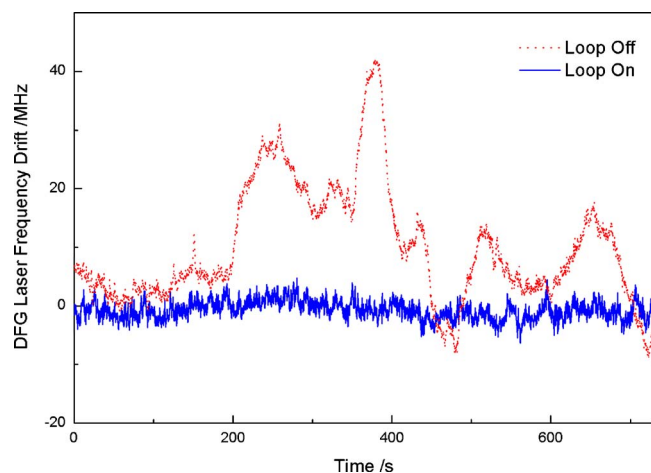

FIG. 3. (Color online) Frequency drift of the DFG emission when the stabilization loop is on (solid line) and off (dash line).

the stability of the DFG emission and allow precise line profile measurement.

C. Spectrum calibration and the data acquisition

The spectrum obtained through scanning the Ti:Sa laser is usually calibrated with a λ-meter or the etalon fringes. But these methods fail for the precise measurement where a few megahertz accuracy is anticipated. The FPI used in the present work has a free spectral range of 1.5 GHz. It is fine to cover a spectrum which spreads over tens of gigahertz, but not adapted to calibrate a line profile with a satisfied precision. Here we use the sidebands produced from the EOM modulation for the calibration purpose.

As shown in Fig. 1, the laser beam going to the FPI (free spectral range of 1.5 GHz) is modulated by a broadband nonresonant EOM2 (LEYSOP). The driving rf signal is generated from a series of voltage-controlled oscillators (VCOs). The rf's are monitored with a rf counter (INSTEK GFC-8270H) with 0.1 MHz accuracy. In present study, two VCOs running at frequencies of 252.2 and 449.0 MHz are applied to generate two sidebands on both sides of the carrier laser frequency. So altogether five markers (±252.2, 0, and ±449.0 MHz) can be used to calibrate the spectrum. The Ti:Sa laser is running in a step-scan mode controlled by the PC. On each step, the DFG signals obtained from the lock-in amplifiers and the FPI signal are recorded simultaneously. The whole scan range covering 1–2 GHz consists in about 500 steps and is finished typically within 100 s to minimize the influence from the long-term drift of the FPI due to the temperature fluctuations. The FPI spectrum will be first used to generate a calibration formula using the rf markers. Then the DFG spectrum will be generated after intensity normalization and spectral calibration.

D. CH$_4$ line profile measurements

The CH$_4$ absorption line at 2927.0762 cm^{-1} is recorded as a test of the DFG apparatus. The CH$_4$ sample gas was purchased from Nanjing Special Gases Factory (stated purity of 99.99%) and used without further purification. 0.15 Torr CH$_4$ gas was filled in a 20.0 cm long quartz cell. The sample pressure was measured with a MKS Baratron manometer (model 627B, full scale 1 Torr, stated accuracy 0.12%). The measurement was carried out at room temperature (300 K). A piece of the spectrum is shown in Fig. 4. Panels (a) and (b) are the FPI spectrum and the sample spectrum, respectively.

The detected spectrum is the convolution product of the absorption line profile and the instrumental function $\phi_I(\nu)$,

$$I(\nu) = [I_0(\nu)e^{-k(\nu_0)NL\phi(\nu)}] \otimes \phi_I(\nu), \tag{1}$$

where L is the absorption path length, N is the molecular density (in molecules/cm^3), and $k(\nu_0)$ is the line strength (in cm^{-1}/molecule cm^{-2}) of the absorption line centered at ν_0. The absorption line profile ϕ can be modeled as a Voigt line shape, in which the Gaussian linewidth [full width at half maximum (FWHM)] value is fixed at the calculated Doppler width 0.009 07 cm^{-1}, and the Lorentzian linewidth is fixed at 1.5×10^{-5} cm^{-1} which is calculated from the self-broadening constant given in the Hitran database.[18] The DFG spectrometer instrumental function can be modeled as
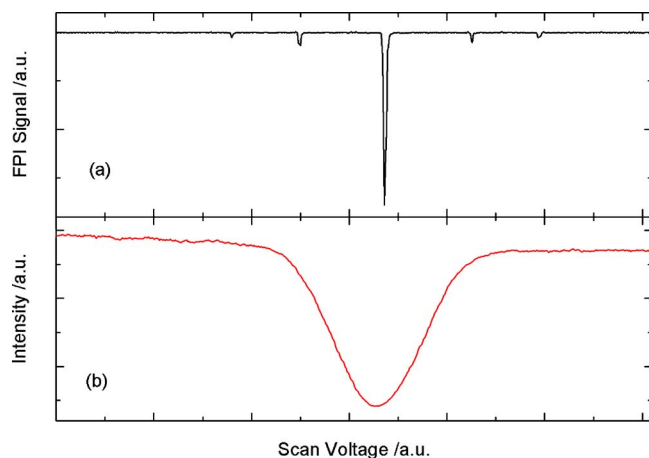
FIG. 4. (Color online) CH_4 line at 2927.0762 cm^{-1} recorded by the DFG spectrometer. (a) FPI spectrum; (b) CH_4 absorption spectrum.

Gaussian, Lorentzian, or Voigt profiles. The instrumental function parameters and the base lines are derived from the simultaneous fitting of about ten spectra obtained from different measurements. From such a least-squares fitting, the best-fitted instrumental function is a Lorentzian function with a FWHM width of 1.7×10^{-4} cm^{-1}. A piece of the observed spectrum and the calculated one are given in Fig. 5. The fitting residuals are also given in the same figure. Note that the main contribution of the linewidth comes from the Doppler width, which has been fixed at the theoretical values in the fitting. The very small difference between the calculated and observed spectrum presents an illusion of the reliability of the spectrometer.

III. DISCUSSION AND PERSPECTIVES

We have set up a mid-IR DFG laser spectrometer for precise molecular spectroscopy measurements. The frequency accuracy is improved to the 1×10^{-4} cm^{-1} level by frequency stabilizing the 1064 nm Nd:YAG laser to the iodine Doppler-broadening absorption line near 532 nm. As discussed in Sec. II, the Nd:YAG laser has been actually stabilized to the 10^{-6} cm^{-1} level, and the present bottle neck
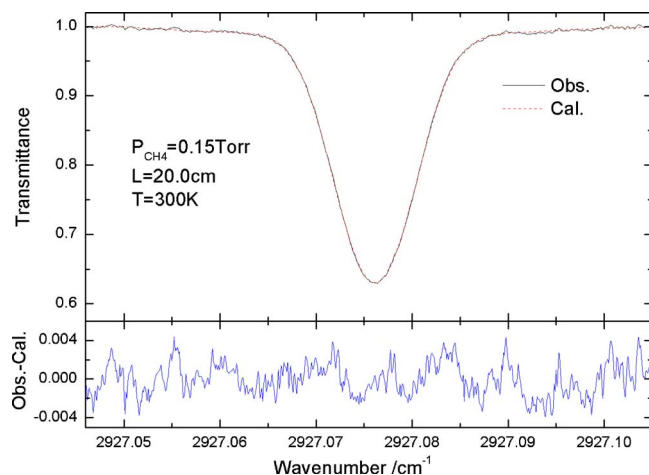
to the further improvement on the frequency accuracy is the stability of the Ti:Sa laser. The present long-term drift of the DFG IR emission, a few megahertz shown in Fig. 3, most probably comes from the drift of the Ti:Sa laser. The performance will be close if the lasers used here are replaced with more compact near-IR diode lasers. Locking the Ti:Sa laser to a frequency-stabilized reference will bring the accuracy to the 10^{-6} cm^{-1} level, but this will make the scanning more complicated when a large scanning range is necessary.

Another possible improvement in present DFG system can be the frequency calibration. Although we have experimentally demonstrated that applying present sidebands calibration method the frequency accuracy can be as good as 1 MHz, the long-term drift of the FPI cavity will be a problem especially in a very long time measurement. Using a stabilized FPI (Ref. 19) will help in solving the problem. Alternatively, the beating signal between the Ti:Sa laser and another frequency-stabilized single mode laser can provide frequency accuracy to the subkilohertz level. Such a mid-IR DFG laser system with kilohertz spectral accuracy can be applied to determine the Boltzmann constant by measuring a molecular absorption line in the mid-IR region. However, the spectral cover range could be much limited in this case. In turn, the present DFG system provides us the possibility to do precise spectroscopy measurement in the whole region of 2.3–5.0 μm. Since many important molecules (including most atmospheric molecules) have strong fundamental absorption bands in this spectral region, and the Doppler/collision induced widths are in the order of 10^{-3}–10^{-2} cm^{-1}, the moderate spectral accuracy of 10^{-4} cm^{-1} is very suitable for the line profile studies of such molecules. Note that the near-IR lasers used in here can be replaced with very compact diode lasers, such a DFG system can be also potentially applied in many field studies, for example, the isotope concentration measurements of atmospheric molecules.

FIG. 5. (Color online) CH_4 line at 2927.0762 cm^{-1}, experimental (solid line), calculated (dash line) and fitting residuals (lower panel).

[1] C. Fischer and M. W. Sigrist, Top. Appl. Phys. **89**, 97 (2003).
[2] D. Mondelain, S. Payan, W. Deng, C. Camy-Peyret, D. Hurtmans, and A. W. Mantz, J. Mol. Spectrosc. **244**, 130 (2007).
[3] D. Mondelain, P. Chelin, A. Valentin, D. Hurtmans, and C. Camy-Peyret, J. Mol. Spectrosc. **233**, 23 (2005).
[4] R. Wehr, J. R. Drummond, and A. D. May, Appl. Opt. **46**, 978 (2007).
[5] K. M. T. Yamada, A. Onae, F.-L. Hong, H. Inaba, H. Matsumoto, Y. Nakajima, F. Ito, and T. Shimizu, J. Mol. Spectrosc. **249**, 95 (2008).
[6] C. Daussy, M. Guinet, A. Amy-Klein, K. Djerroud, Y. Hermier, S. Briaudeau, C. J. Borde, and C. Chardonnet, Phys. Rev. Lett. **98**, 250801 (2007).
[7] F. K. Tittel, D. Richter, and A. Fried, Top. Appl. Phys. **89**, 445 (2003).
[8] J. S. Balent, Jr. and A. W. Mantz, Appl. Opt. **31**, 1907 (1992).
[9] A. Valentin, Spectrochim. Acta, Part A **52**, 823 (1996).
[10] A. Vitcu, R. Ciurylo, R. Wehr, J. R. Drummond, and A. D. May, Appl. Opt. **43**, 4965 (2004).
[11] J. A. Armstrong, N. Bloembergen, J. Ducuing, and P. S. Pershan, Phys. Rev. **127**, 1918 (1962).
[12] L. H. Deng, X. M. Gao, Z. S. Cao, W. D. Chen, Y. Q. Yuan, W. J. Zhang, and Z. B. Gong, Opt. Commun. **268**, 110 (2006).

[13] D. Mazzotti, P. De Natale, G. Giusfredi, C. Fort, J. A. Mitchell, and L. W. Hollberg, Appl. Phys. B: Lasers Opt. **70**, 747 (2000).

[14] Y.-R. Shen, *Nonlinear Infrared Generation* (Springer, Berlin, 1977), pp. 25–36.

[15] M. L. Eickhoff and J. L. Hall, IEEE Trans. Instrum. Meas. **44**, 155 (1995).

[16] K. Nyholm, M. Merimaa, T. Ahola, and A. Lassila, IEEE Trans. Instrum. Meas. **52**, 284 (2003).

[17] D. W. Allan, Proc. IEEE **52**, 211 (1966).

[18] L. S. Rothman, D. Jacquemart, A. Barbe, D. Chris Benner, M. Birk, L. R. Brown, M. R. Carleer, C. Chackerian, Jr., K. Chance, V. Dana, V. M. Devi, J.-M. Flaud, R. R. Gamache, A. Goldman, J.-M. Hartmann, K. W. Jucks, A. G. Maki, J. Y. Mandin, S. T. Massie, J. Orphal, A. Perrin, C. P. Rinsland, M. A. H. Smith, J. Tennyson, R. N. Tolchenov, R. A. Toth, J. Vander Auwera, and P. Varanasi, J. Quant. Spectrosc. Radiat. Transf. **96**, 139 (2005).

[19] A. Rossi and V. Biancalana, Rev. Sci. Instrum. **73**, 2544 (2002).